Reaction Layers and Mechanisms for a Ti-Activated Braze on Sapphire

J.J. STEPHENS, F.M. HOSKING, T.J. HEADLEY, P.F. HLAVA, and F.G. YOST

A study was conducted to understand the wetting phenomena observed in brazing of a Ti-containing active filler metal on sapphire substrates. The goal of the study was to understand the interfacial reactions that permit wetting of commercial Ag-Cu-Ti active filler metal to pure alumina, despite the lower thermodynamic stability of TiO_2 relative to Al_2O_3. Based upon transmission electron microscope, electron microprobe, and Auger analyses, it is proposed that two coupled reactions and diffusion of reactants take place. The oxides TiO, Ti_2O, and Cu_3Ti_3O were observed at the braze/ceramic interface. It is suggested that the complex oxide Cu_3Ti_3O grows at its interface with TiO, and the oxide TiO is produced by reaction of Ti and sapphire and is subsequently consumed at its interface with Cu_3Ti_3O. It is also suggested that Ti_2O forms from Ti and TiO while cooling from the brazing cycle.

I. INTRODUCTION

BRAZE alloys containing small amounts of an active metal, commonly referred to as active braze alloys (ABAs), are often used to join ceramics to metals and ceramics to ceramics. Active metal brazing results in considerable cost savings by means of simplified production sequences and more efficient mechanical designs. Most notably, ABA filler metals have the potential to eliminate the need for Mo-Mn metallization and the subsequent Ni plating of alumina surfaces prior to brazing, which is a standard industrial process. The active constituent is often Ti, but other reactive metals such as Nb, V, Zr, or Hf are also suitable constituents. The bond developed by these braze alloys stems from the reaction that occurs between the active constituent and the ceramic while the alloy is in the molten state. That thin reaction layer allows the molten alloy to wet the ceramic surface, resulting in the joining of mating surfaces. Note that ABAs spread only as a result of chemical reaction with the ceramic surface. Several commercially available filler metals exist, based upon Cu, Ag, Ni, or Au, that contain one of the active constituents for joining ceramic materials.

The successful ABA joint requires the selection of an active constituent such that the chemical reaction with the mating ceramic surface yields a uniform and continuous reaction layer. In addition, the brazing-process thermal cycle and atmosphere must be properly controlled, in particular to prevent unwanted dissolution and chemical reactions at the mating metal or ceramic surface.

At present, commercial ABA filler metals typically have Ti as the active constituent. The most widely used composition is 63 wt pct Ag, 35.25 wt pct Cu, and 1.75 wt pct Ti (known by the trade name CusilABA, which is produced by WESGO Metals, Inc. (Hayward, CA)). For many applications, Ti is an excellent active element because it reacts with many metallic and nonmetallic surfaces. However, there are certain alloy surfaces such as KOVAR,* a low-expansion Fe-Ni-Co alloy used extensively in electronic applications, that scavenge Ti from the ABA filler metal, thus resulting in nonhermetic joints and some loss in joint strength.[1] As a result, it is important to carefully choose the active metal and thoroughly understand the chemical reactions involved.

*KOVAR is a trademark of Carpenter Technology Corporation, Reading, PA.

The brazing of 94 pct grade alumina (balance CaO-MgO-SiO_2) ceramic to itself or to metal substrates with a Ti active braze is typically done with the ceramic surface air fired (*e.g.*, 2 hours at 1575 °C) prior to brazing. The air-firing cycle permits silica from the glassy phase to diffuse to the surface and to heal any grinding-induced microcracks in the ceramic. Titanium-containing ABAs react very well with alumina substrates containing a grain-boundary silicate phase.[2] The amount of this phase, *i.e.*, the percent purity of alumina, is not a critical parameter. However, it has not been determined for certain whether Ti-containing ABAs can wet sapphire—that is, alumina in the absence of the glassy silicate phase(s).

It has been shown by Selverian *et al.*[3] that vapor-deposited Ti reacts with R-plane ($(1\bar{1}2)$ in rhombohedral notation or $(2\bar{3}12)$ in hexagonal notation) oriented sapphire substrates. While the Ti was strongly textured in the as-deposited condition, no lattice matching with sapphire was observed. In addition, no lattice relationship with reactant phases was noted. The reaction between Ti and sapphire was suggested to be

$$\mathrm{Ti} + \frac{1}{8}\mathrm{Al_2O_3} \rightarrow \frac{3}{8}\mathrm{Ti_{0.67}[O_{0.33}]} + \frac{1}{4}\mathrm{Ti_3Al[O]} \quad [1]$$

where the reactant phases are solid solutions of Ti plus O and Ti_3Al plus O. Selverian *et al.* suspected that the partial pressure of oxygen may play an important role in this reaction. A limited thermodynamic analysis of this reaction can be found in References 3 and 4. In similar experiments on 95 pct alumina, Kang and Selverian[5] found the same Ti_3Al phase as well as a Ti_5Si_3 phase due to the reaction between Ti and the glassy grain-boundary phase.

J.J. STEPHENS, F.M. HOSKING, T.J. HEADLEY, and P.F. HLAVA, Principal Member of Technical Staff, are with Materials and Process Sciences (1800), Sandia National Laboratories, Albuquerque, NM 87185. Contact e-mail: jjsteph@sandia.gov F.G. YOST, President, is with Trapezium Technology, Albuquerque, NM 87107.

Manuscript submitted January 17, 2003.

Santella *et al*.[6] brazed a CuAgSnTi alloy to an alumina substrate and found a two-layer reaction zone. This zone consisted of a 2 to 3-μm-thick equiaxed layer of Cu_3Ti_3O with trace amounts of Al and a thin 0.1 to 0.2-μm-thick layer of γ TiO having elongated grains. Note that Sn had no apparent role in the reaction layer. Carim[7] used a commercial AgCuTi alloy, with a composition corresponding to CusilABA, on sapphire substrates and also found a $(Cu, Ti, Al)_6O$ phase, but made no mention of the γ TiO phase. The brazing process used in Reference 7 consisted of a vacuum atmosphere and braze-process cycle consisting of 10 minutes at a peak temperature of 1098 K.

More recent studies[8–11] have shed additional light on the reaction(s) between Ti-containing ABAs and alumina. Kelkar *et al*. have demonstrated the thermodynamic possibility of Reaction 8 and also estimated the solubility of Al in the oxide Cu_3Ti_3O to be as high as 15 at. pct.[9] Furthermore, they suggest that Al substitutes for Cu in the crystal structure of Cu_3Ti_3O. Hao *et al*.[10] suggested that at and above 1123 K, Ti reacts at the alumina interface to form the phase $CuTi_2$ and a mixed layer of TiO and Ti_2O. Ichimori *et al*.[11] examined the reaction of sapphire with a 66.7 wt pct Ag-28.4 wt pct Cu and 4.9 wt pct Ti filler metal brazed in vacuum at a peak temperature of 1173 K for 300 seconds using transmission electron microscopy (TEM). They observed a typical interfacial structure of Ag-Cu eutectoid/Ti_3Cu_3O ($\sim$1 to 2-μm thick)/TiO(10 to 50-nm thick)/sapphire for all the orientations of sapphire examined. However, they also observed isolated areas where the Ti_3Cu_3O was present without the TiO interlayer and an occasional reaction phase without Ti concentration, a Cu-Al-O phase, in direct contact with the sapphire substrate.

The objective of the present work is to investigate a Ti-bearing ABA and its reaction with sapphire substrates. The use of sapphire substrates eliminates the possibility of extraneous reactions with the grain-boundary silicate phase found in polycrystalline alumina substrates. The brazing conditions of time and temperature are chosen to simulate those of a commercial process. It is realized that the short brazing times employed here may prevent the formation of equilibrium phases, and this will make it difficult to compare results with those reported in the literature. However, it is important to understand the phase development that results from commercial processes. The brazements are examined to determine phase identity, morphology, and constituency, and these findings are compared with previous work. The formation mechanism of these phases is then proposed.

II. EXPERIMENTAL PROCEDURE

A. *Materials Preparation and Brazing Process*

The braze alloy, CusilABA, was utilized for this investigation. WESGO Metals supplied the material in 5.08-cm-wide strip form, with a thickness of 0.076 mm. Table I shows the chemical-analysis information supplied by WESGO Metals for the specific lot (number 89186) of commercially available material used in this study. While the chemistry of commercial products from WESGO Metals is well controlled, the behavior of corresponding products from other vendors is beyond the scope of this study. Round disks of CusilABA with a diameter of 10.2 mm were punched from the strip material in order to perform braze wetting experiments. The sapphire substrates had a basal-plane orientation, 12.7 mm diameter, with a thickness of 1 mm, and an optically polished surface finish. They were supplied by the Swiss Jewel Company (Philadelphia, PA). Prior to the braze process, the substrates were air fired for 2 hours at 1848 K in a covered alumina boat to help remove any residual hydrocarbons from the polishing process.

Table I. Chemical Composition (Weight Percent) of CusilABA Alloy, Lot 89186, Supplied by WESGO Metals

Major elements					
Ag	64.18	Cu	34.09	Ti	1.73
Minor elements					
Au	0.001	Cd	0.0004	Zn	0.0006
Co	0.004	Cr	0.0002	Ge	0.003
In	0.01	Fe	0.002	Mo	0.008
Si	0.002	Y	0.001	C	0.0110
N	0.0010	O	0.0010		

Duplicate wetting samples were fabricated. All brazing processes were performed in dry hydrogen. The brazing was performed in a Centorr Model 17 bottom-loaded furnace equipped with a tungsten-mesh heating element. As a cautionary procedure, ultrahigh-purity hydrogen gas, supplied from a cylinder bank and passed through a Pt-Pd catalyst and moisture dessicator, was supplied to the furnace atmosphere at room temperature. This particular gas-scrubbing process results in a hydrogen atmosphere with a typical input dew point of -60 °C. The furnace was controlled with an Inconel-sheathed (Omega Engineering, Inc., Stamford, CT) chromel-alumel (type K) thermocouple, 1.6 mm in diameter, that was fixtured close to the wetting samples in order to ensure that the sample temperatures were very close to the control temperature. The following process cycle was used: heat from room temperature to 1003 K at a rate of 15 °C/min, hold 15 minutes at 1003 K, heat at 10 °C/min to 1118 K, hold 6 minutes at 1118 K, followed by a furnace cool to room temperature.

B. *Analytical Procedures*

It was anticipated that the reaction layer(s) would be quite thin, because of the short brazing cycle. Therefore, TEM was performed to identify all reaction phases at the braze/ceramic interface, using electron diffraction and X-ray energy-dispersive spectroscopy (EDS) semiquantitative analysis. Electron microprobe analysis (EMPA) and auger electron spectroscopy (AES) were used to support the TEM evaluation. Following braze processing, one sample was used for TEM analysis, while the other sample was metallographically cross sectioned for EMPA. The sample for TEM analysis was lapped at a shallow angle through the braze metal, reaction zone, and sapphire substrate and then polished. A thin cross section through the entire reaction zone was extracted with the use of a focused ion beam (FIB) instrument. The thin section was placed on a carbon substrate on an aluminum grid and examined in a PHILIPS* CM30 transmission electron microscope operating at 300 kV and equipped with an Oxford Instruments EDS spectrometer. Typical EDS probe diameters

*PHILIPS is a trademark of Philips Electronic Instruments Corp., Mahwah, NJ.

used were 40 nm for spot-mode analyses and 25 nm for automated-profile-mode analyses.

Auger electron spectroscopy (AES) was performed on Cu_3Ti_3O in the reaction zone of the shallow-lapped sample by sputtering into the phase. The analysis was done in a Physical Electronics (Minneapolis, MN) model PHI680 scanning auger microprobe with a 5 keV, 20 nA electron beam. Sputtering was done using a 1×1 mm raster xenon ion beam at 2 keV and 0.5 μA.

For EMPA, pieces were cross sectioned, mounted in epoxy, metallographically prepared, and carbon coated. These were examined with a JEOL* JXA-8600 electron microprobe operated in the wavelength-dispersive mode for both photomicrography and quantitative analytical traces. In addition to backscattered electron (BSE) images, semiquantitative element maps were obtained with the referenced elemental concentration, by weight, noted on the individual map legend. The instrument was operated using a Tracor–Northern automation package and SandiaTask software (phi-rho-z corrections for quantitative analyses).[12] Calibration of the elements of interest used pure-element standards except for oxygen, which used a previously analyzed, natural hematite (Fe_2O_3) standard.

*JEOL is a trademark of Japan Electron Optics Ltd., Tokyo.

III. RESULTS

A. *Reaction-Layer Microstructure*

Sapphire substrates wetted with the CusilABA alloy were sectioned and polished for EMPA examination. Figure 1(a) shows a BSE image of the cross section of one such specimen. The filler metal is located at the top and the sapphire substrate at the bottom of this photomicrograph. Recognizing resolution limits in the EMPA of approximately 1 μm (governed by the volume irradiated by the electron beam), the six parts of Figure 1 suggest that there is only one phase resulting from the reaction between the ABA and sapphire. Furthermore, Figure 1(b) suggests that oxygen is a minor, but uniformly distributed, constituent of the reaction layer. Figures 1(c) and (d) show that Ag is confined to the braze region, while Cu is a significant component of both the braze region and reaction layer. Figure 1(e) suggests that Al is confined to the substrate, and Figure 1(f) shows Ti to be a significant component of the reaction layer, but also seems to be dissolved in the Cu-rich regions of the braze. For example, the large globular Cu-rich phase apparent in the right-hand side of Figure 1(a) has a noticeable Ti content (Figure 1(f)).

Figure 2 shows an EMPA line analysis of Cu, Ag, Ti, Al, and O taken perpendicularly through the reaction zone. It is one of seven traces taken of this particular sample and is characteristic of the set. It clearly shows the braze and sapphire regions and a reaction layer that is approximately equiatomic in Cu and Ti. Also evident is a tail in the Al distribution that extends well into the reaction layer. It cannot be claimed, without some doubt, that this tail is due to Al diffusion into the reaction layer. The tail could also be caused by the X-ray sampling volume of the electron beam. However, the Al X-ray map of this region, and also in that of the other six traces [not shown], indicates some Al activity in the reaction layer.

Three Ti-bearing phases were identified by TEM in the reaction layer, as shown in Figure 3. A thin layer of crystalline γ TiO is continuous and appears to completely cover the sapphire interface. The major phase above the γ TiO layer is a coarser-grained layer averaging ~2.2-μm thick. This phase is Cu_3Ti_3O. A third phase occurs discontinuously between the γ TiO and Cu_3Ti_3O layers and was identified as Ti_2O. The linear fraction of Ti_2O at this interface was found to vary widely, from approximately 5 to 80 pct over the length of interface examined using TEM. Note that it is very easy to confuse the identification of Cu_3Ti_3O with that of $CuTi_2$ from electron-diffraction analysis alone. Other techniques (such as AES) that detect the oxygen are helpful to verify the identity of the compound.

B. *The TEM and AES Analyses*

Figure 4 is a higher-magnification image of the thin TiO layer at the sapphire interface. This layer is polycrystalline and its thickness varies from ~20 to ~200 nm, with a mean value of ~100 nm. The layer was continuous over the entire length (~50 μm) of interface examined using TEM. The EDS spectrum of this phase showed Ti and O peaks as well as an Al peak. The Al peak arises from either spurious fluorescence of the Al TEM grid supporting the thin FIB slice or from its natural presence in the cross section. The crystal structure of this phase was identified by electron diffraction as γ TiO (fcc, $Fm\bar{3}m$, NaCl-structure-type, measured $a_o = 0.419$ nm). Figure 5 shows the [110] zone-axis pattern.

The crystal structure of the coarser-grained phase above the γ TiO layer (Figure 4) was identified from electron diffraction as that of Cu_3Ti_3O (diamond-cubic, $Fd\bar{3}m$, CFe_3W_3-structure-type, measured $a_o = 1.137$ nm). Figures 6(a) and (b) show the [110] and [100] zone-axis patterns, respectively. The EDS spectrum from this phase showed strong Ti and Cu peaks and small Al and O peaks. The O peak in that EDS spectrum was quite small, so the O content of this phase was probed by AES, which showed a significant O signal. Quantitative analysis of the AES spectrum gave an O content of about 12 at. pct, which compares favorably with 14.3 at. pct for stoichiometric Cu_3Ti_3O. Kelkar *et al.*[8] reported that this phase accommodates Al, substituting for Cu, up to a limit corresponding to Cu_2AlTi_3O. In the present work, AES analyses taken across this phase in the inclined, lapped sample indicated an Al diffusion profile, although quantification was not reliable. Therefore, the Al, Ti, and Cu contents were quantified across the Cu_3Ti_3O layer by EDS analysis using TEM on an additional FIB slice that was supported on a Ni grid. This avoided spurious contribution to the Al, Ti, and Cu signals. Profiles at ~0.1-μm steps were obtained from two different traces across the layer. The results are shown in Figures 7 and 8. The oxygen content in these profiles was not quantified and was assumed to be 14.3 at. pct for stoichiometric Cu_3Ti_3O. The TEM micrographs showing the respective paths of the two profiles are shown in Figures 9 and 10. The EDS analysis indicated negligible Al and Ti contents in both the Ag-rich and Cu-rich phases of the braze metal at locations just above the Cu_3Ti_3O layer (within 0.1 μm of the interface).

Recall that initial quantitative results on the Al content of Cu_3Ti_3O were obtained by EMPA and were held suspect.

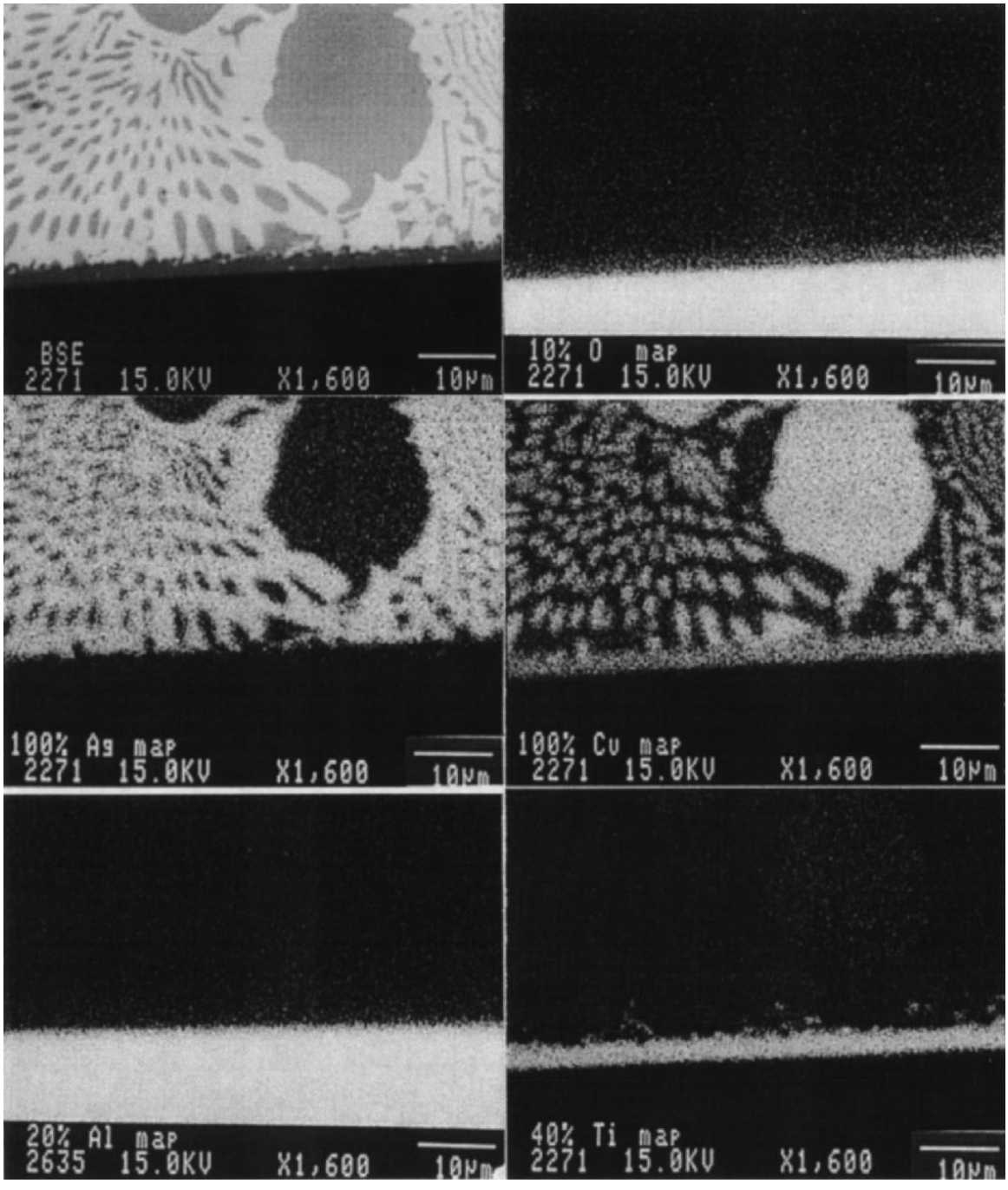

Fig. 1—BSE image and semiquantitative element maps of a wetting sample of CusilABA on a basal plane sapphire substrate. The sapphire is at the bottom of the micrograph. The sample was brazed in dry H_2 using a process profile with a peak temperature of 1118 K for 360 s. Each map is labeled in the lower-left-hand corner as to the nominal dot density (weight percent) used to obtain the image. The aluminum and oxygen maps were taken at extended exposure conditions to reveal the low concentrations found in the reaction layers: (*a*) BSE image of braze section, (*b*) 10 pct oxygen X-ray map, (*c*) 100 pct Ag X-ray map, (*d*) 100 pct Cu X-ray map, (*e*) 20 pct Al X-ray map, and (*f*) 40 pct Ti X-ray map.

Follow-up measurements by AES and EDS support the conjecture that the diffusion-like tail of Al in this phase is real and not due to beam overlap or some other artifact of the analytical technique. The Al must come from reduced Al_2O_3 diffusion through the TiO and into the Cu_3Ti_3O. Figure 7 shows that at the TiO interface, the Al content is approximately 5 at. pct, while at the ABA interface, it is slightly less than 2 at. pct. It could be higher at the interface, but the resolution was insufficient. Two different measured profiles, from separate regions of the same sample, seem to agree within a small error. Figure 8 indicates that a diffusion profile also exists for Cu diffusing in the opposite direction. At the ABA interface, the Cu content is approximately 45 at. pct, while at the TiO interface, it is 41 to 42 at. pct. Two Ti profiles do not indicate long-range diffusion gradients, although short fluctuations may be present. The EMPA

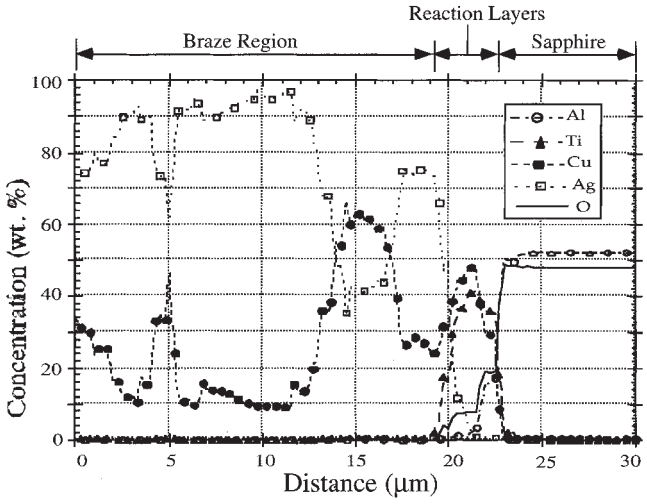

Fig. 2—EMPA line analysis showing approximate chemistries for Cu, Ag, Ti, Al, and O.

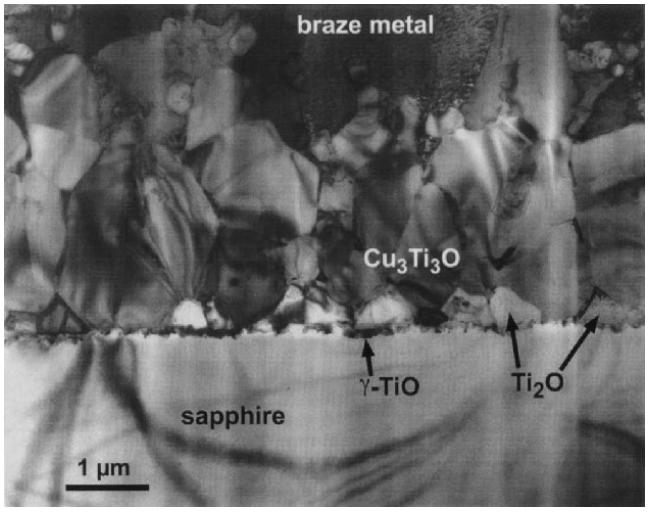

Fig. 3—TEM cross section of reaction phases at braze metal/sapphire interface.

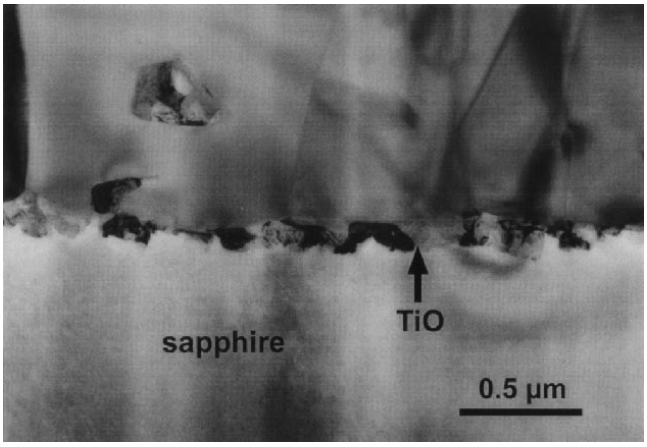

Fig. 4—Thin, continuous, polycrystalline TiO layer (arrow) at the sapphire interface.

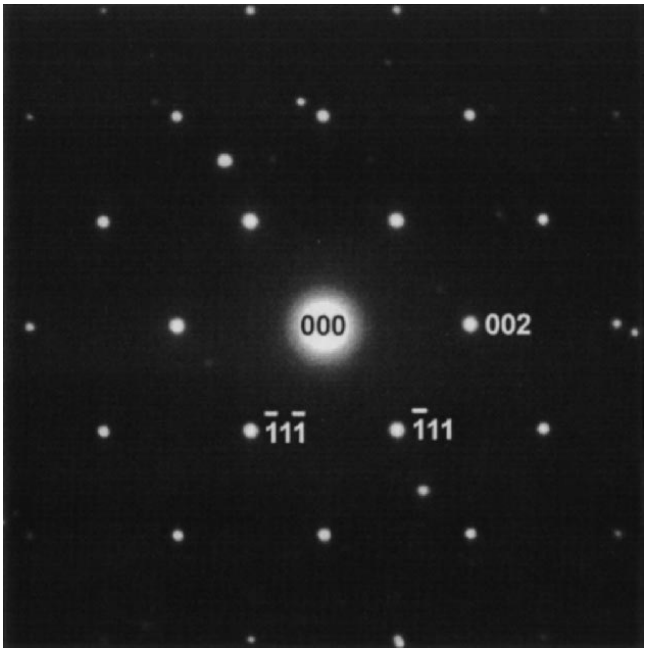

Fig. 5—[110] zone-axis electron-diffraction pattern of γ TiO (fcc, NaCl structure type). Extra spots arise from portions of adjacent grains within the selected-area aperture.

shown in Figure 2 also suggests that an oxygen diffusion tail is present and may, in fact, track that of Al. However, the measurement of oxygen content is unreliable without sufficient resolution. It could be higher, as Kelkar *et al.*[8] suggested, but not within the profiles measured in this study.

Figure 11 shows a single grain of the Ti_2O phase at the γ TiO-Cu_3Ti_3O interface at a location where small amounts of Ti_2O were observed (compare Figures 3 and 11). The corresponding EDS spectrum is shown in Figure 12. (The small Al and C signals are artifacts arising from the Al grid bar and carbon substrate, respectively). Although the oxygen signal is very low in this spectrum, electron-diffraction analysis of this phase identified the crystal structure as that of Ti_2O (rhombohedral, $P\bar{3}m1$, CdI_2-structure-type, and space group 164).

Figure 13 shows the $[11\bar{2}0]$ and $[10\bar{1}0]$ electron diffraction patterns from this phase (based on a hexagonal cell). The presence of hkil reflections, for which l = odd in the $[10\bar{1}0]$ pattern, distinguishes the rhombohedral Ti_2O structure from that of hcp α Ti, which does not contain these reflections in the $[10\bar{1}0]$ pattern. To investigate the stability of the Ti_2O phase, an additional vacuum anneal for 7 hours at 773 K was given to two specimens, initially containing 5 and 75 pct linear fractions of Ti_2O, respectively. The first specimen showed an increase to between 40 and 50 pct linear fractions of Ti_2O, while the second specimen showed no noticeable increase. The influence of the existence and preponderance of Ti_2O on mechanical properties and the effect of cooling rate on the stability of Ti_2O were beyond the scope of this work.

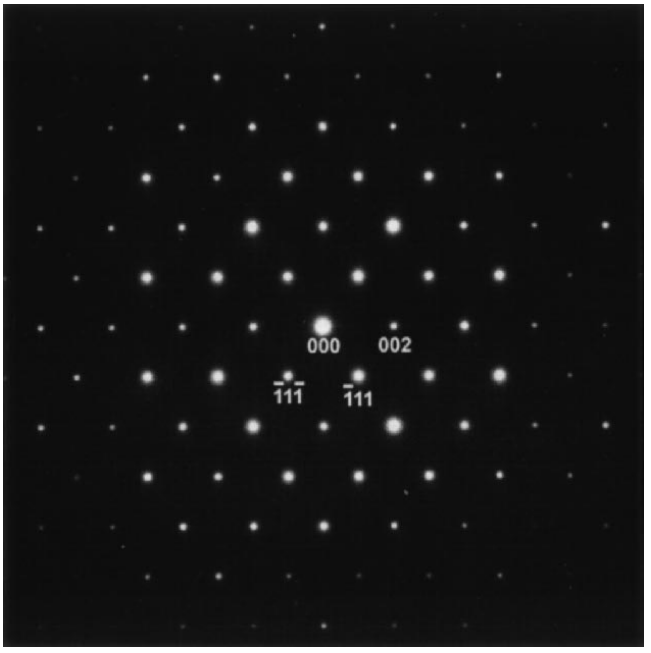

(*a*)

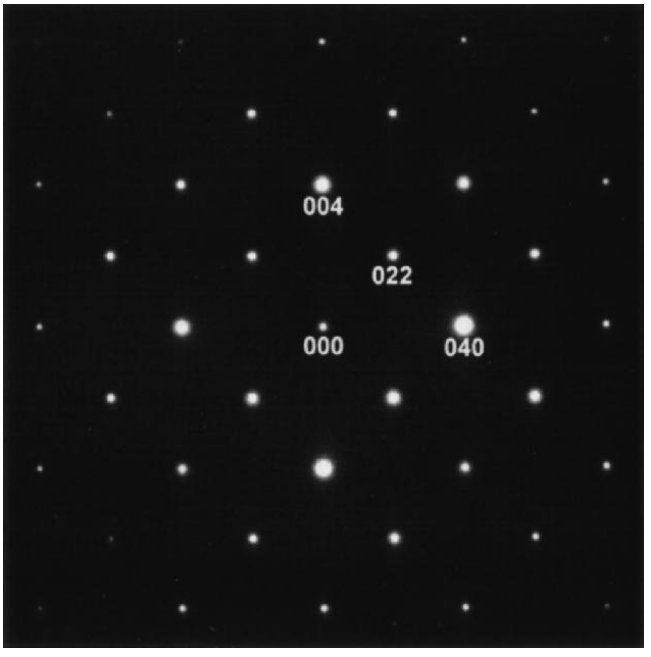

(*b*)

Fig. 6—(*a*) [110] and (*b*) [100] zone-axis electron-diffraction patterns of Cu_3Ti_3O (diamond-cubic, CFe_3W_3 structure type).

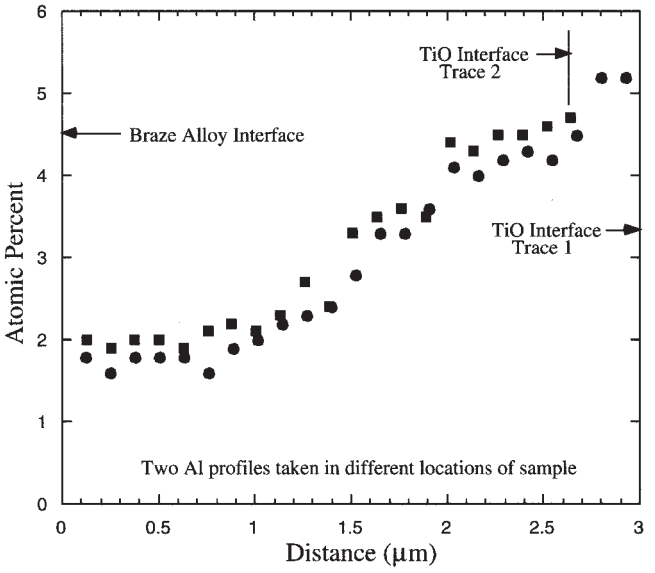

Fig. 7—Two different Al profiles taken by EDS in the same sample.

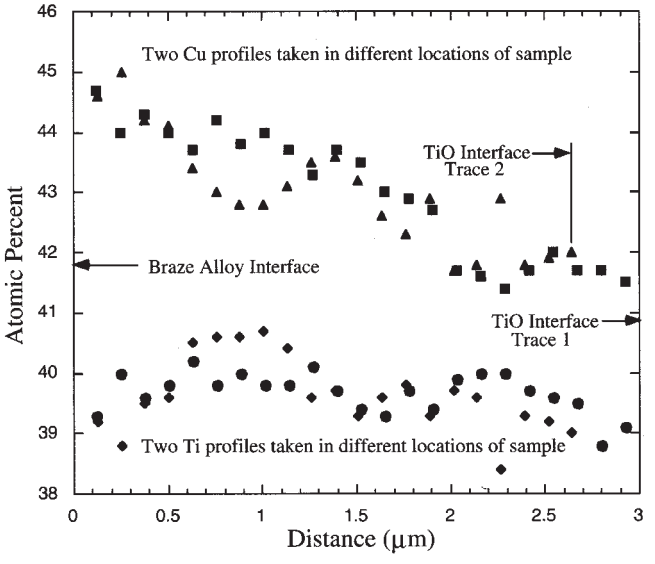

Fig. 8—Two different Cu and Ti profiles taken by EDS in the same sample.

IV. DISCUSSION

A. *Microstructural Analysis*

Brazing experiments with CusilABA and basal-plane-oriented sapphire were performed utilizing a braze cycle having a maximum temperature of 1118 K and a time at peak temperature of 360 seconds in dry hydrogen. It was shown that the resulting reaction layer consists of three phases all containing oxygen and titanium. Only one of the phases, Cu_3Ti_3O, contains Cu in any significant amount. This phase was by far the thickest and was found to have a diamond-cubic lattice. The other phases were γ TiO, which was thin but continuous over the interface and was determined to have an fcc (NaCl) lattice, and Ti_2O, which was found only in isolated regions of the interface and has a rhombohedral lattice. These observations are in essential agreement with the literature,[6–10] although Ti_2O has not always been cited.

Data collected by EDS, EMPA, and AES provided evidence for the presence of a diffusion tail of Al into the reaction layer and away from the sapphire substrate. Indeed, Kelkar and Carim[9] have shown that Cu_3Ti_3O can dissolve significant amounts of Al in solid solution, and Lee and Saunders[13] have predicted that significant solid solubility for Al exists over large portions of the Ti-Al-O ternary-phase

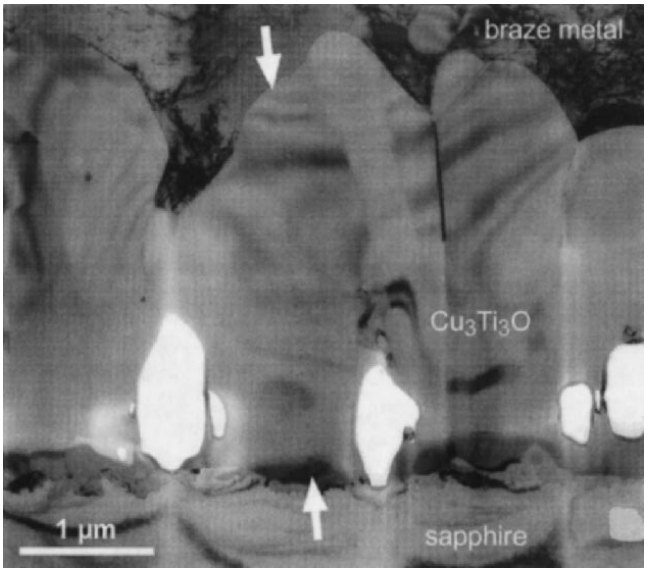

Fig. 9—Location of trace (arrows) for profile 1 across the Cu_3Ti_3O layer.

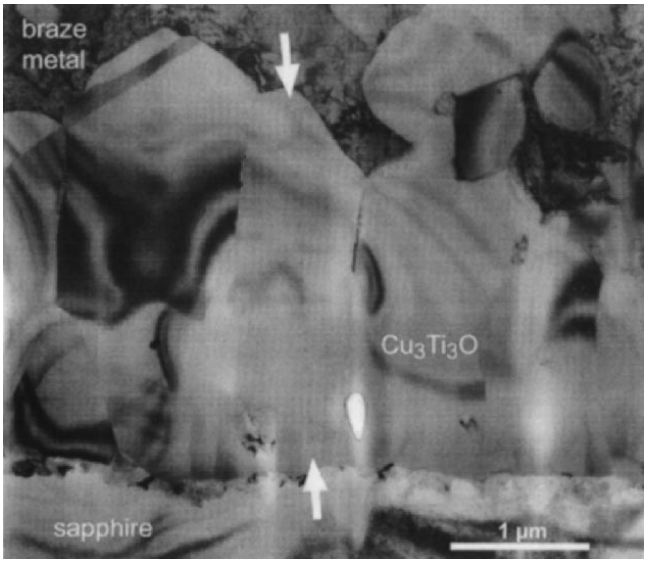

Fig. 10—Location of trace (arrows) for profile 2 across the Cu_3Ti_3O layer.

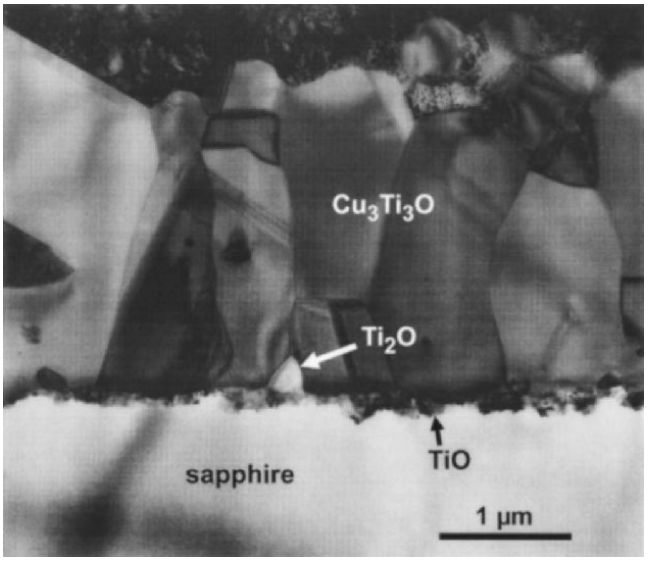

Fig. 11—Single grain (white arrow) of Ti_2O phase at the TiO/Cu_3Ti_3O interface.

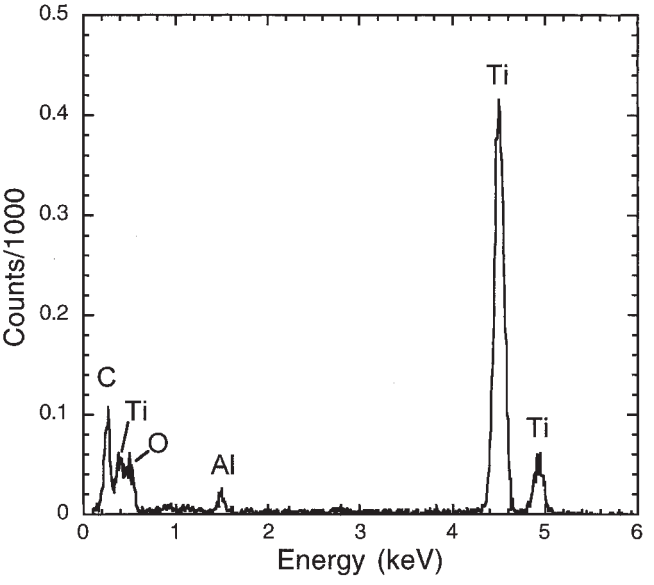

Fig. 12—X-ray EDS spectrum of a grain of the Ti_2O phase.

diagram. The presence of a Cu diffusion tail suggests that Al substitutes for Cu in the Cu_3Ti_3O lattice, which is in agreement with Kelkar and Carim. The lack of evidence for a Ti diffusion tail suggests that it diffuses much more rapidly than Cu and Al (Figure 8).

As shown in Figure 11, Ti_2O occurs only at the Cu_3Ti_3-TiO interface and in singular grain form, with two of its interphase boundaries converging into a Cu_3Ti_3O grain boundary. According to the Ti-O binary-phase diagram,[14] this phase is unstable above approximately 873 K. This suggests that Ti_2O may nucleate upon cooling from the brazing cycle. Titanium from the braze region can diffuse rapidly along Cu_3Ti_3O grain boundaries to the TiO layer, where it can react to form Ti_2O. No thermodynamic information on Ti_2O could be found to corroborate this idea.

Crystallographic data obtained from *Pearson's Handbook*[15] were used to compute the unit-cell volumes of Ti, TiO, and Ti_2O. The volumes of Ti and TiO crystal structures, each containing 1 Ti atom, were found to be 18.07 and 18.39 $Å^3$, respectively. The volume of Ti_2O containing 2 Ti atoms is 36.74 $Å^3$, which represents a volume expansion of 0.28 cubic angstroms. This slight expansion is not expected to cause excessive residual stress due to phase transformation.

B. *Reaction-Layer Formation Process*

When molten metal wets solid metal or ceramic, it is facilitated by a chemical reaction. Equilibrium thermodynamic analysis of potential reactions often serves as a useful predictor of the actual reaction. It is clear from the brazing literature that the reaction chemistry for Ti and alumina may be complex. The displacement reaction between Ti and alumina does not proceed at the brazing temperature, but,

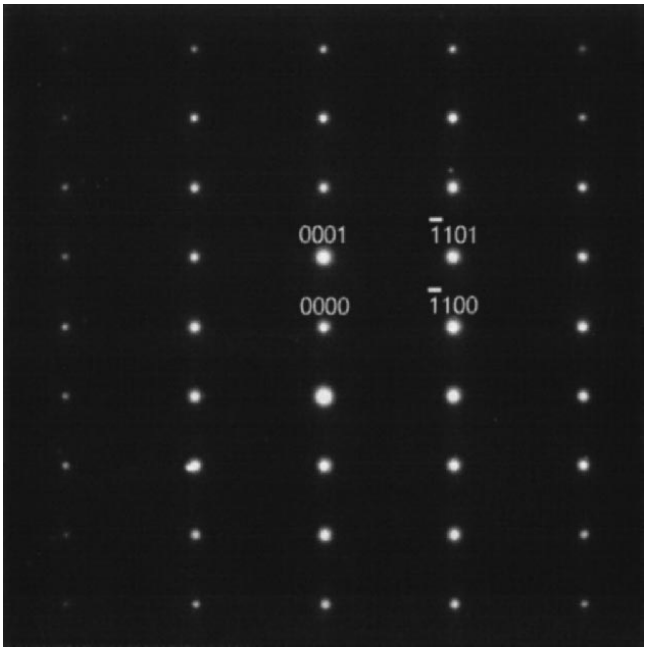

(*a*)

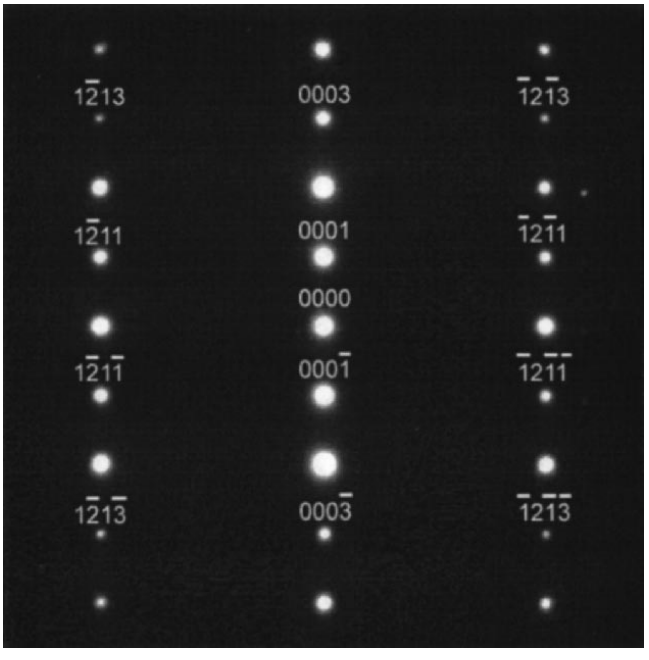

(*b*)

Fig. 13—(*a*) [11-20] and (*b*) [10-10] zone-axis electron-diffraction patterns of Ti_2O (rhombohedral, CdI_2 structure type), zone axes indexed on basis of a hexagonal cell.

in fact, wetting does occur. In addition, the free energy of the reaction

$$\text{Ti} + \frac{1}{3}\,\text{Al}_2\text{O}_3 \rightarrow \text{TiO} + \frac{2}{3}\text{Al} \qquad [2]$$

is positive and approximately 4.66 kJ/mole of Ti at the brazing temperature of 1118 K. According to Kelkar, *et al*.,[8] Cu_3Ti_3O is a very stable oxide with a reaction free energy

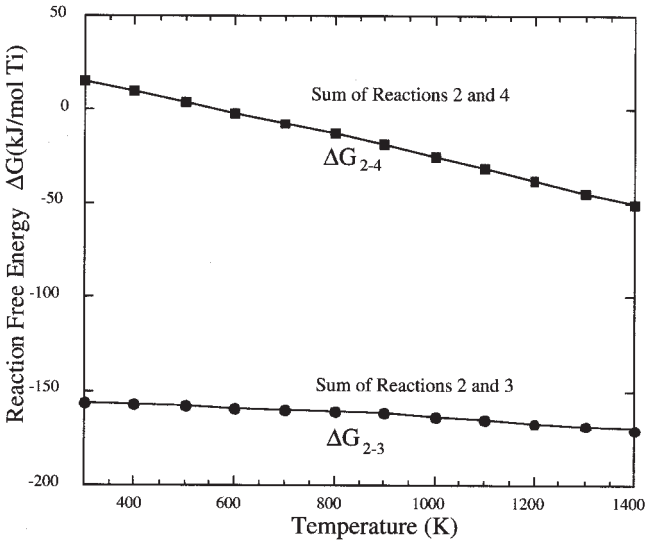

Fig. 14—Summation of reaction free energies for Eqs. [2] + [4] (top curve) and Eqs. [2] + [3] (lower curve). Note: both calculations assume a reaction free energy ($\Delta G_{\text{formation}}$) for Cu_3Ti_3O equal to −170 kJ/mole of Ti. The Appendix provides details.

of approximately −170 kJ/mole of Ti. The formation reaction for this compound can be written as

$$\text{Cu} + \text{Ti} + \frac{1}{6}\,\text{O}_2 \rightarrow \frac{1}{3}\,\text{Cu}_3\text{Ti}_3\text{O} \qquad [3]$$

and the reaction free energy for Reaction [3], when added to that of Reaction [2], produces an overall negative value, implying that the conditions for wetting are favorable and will occur at all temperatures above the melting point of the ABA. The summation of these free energies is shown in Figure 14, and the details of these calculations are shown in the Appendix. Because no further thermodynamic information on Cu_3Ti_3O could be found, it was assumed that the Kelkar *et al*. estimate is independent of temperature. Note that this free energy is computed on a per-mole-Ti basis for each equation (Eqs. [2] and [3]). As shown previously, the Cu_3Ti_3O phase occupies the preponderance of the reaction-layer thickness, so partitioning the total reaction free energy will not reverse the stability of this reaction set. The reaction free energies computed here are approximate, as they do not include various dissolution energies.

The set of Reactions [2] and [3] do not sufficiently describe the reaction process. Since the two product phases are continuous across the interfaces, the reactions producing them should be consecutive and coupled, *i.e*., the reactant in one reaction being the product of another. Reactions [2] and [3] are not coupled, since there is no reactant/product correspondence. Also, it is not clear how and where the oxygen in Reaction [3] is provided. In the following paragraphs, an attempt is made to clarify the reaction processes occurring at the two interfaces bounding the Cu_3Ti_3O phase.

Cited literature and the analytical results presented here suggest that Ti reacts with sapphire and that the product phases Cu_3Ti_3O and TiO are produced during the brazing cycle. At 1118 K, it should be expected that Ti and Cu can diffuse rapidly through liquid ABA to the sapphire surface.

What is not clear, either from the literature or the measurements reported here, is whether oxygen is present in the reaction layers in other than stoichiometric amounts. The oxygen X-ray is weak (<1 KeV) and subject to poor spatial resolution, extensive convolution, interference by other elements present, and other problems. The oxygen trace shown in Figure 2 suggests a concentration gradient. However, the presence of that gradient cannot be stated with certitude. Consequently, it will be assumed that oxygen is stoichiometric and does not diffuse through the reaction layers.

It is suggested that at the initial ABA/sapphire interface, Reaction 2 between Ti and alumina produces TiO and Al. At least one more reaction is necessary to drive the production of TiO, since its free energy of formation is positive at the brazing temperature. This reaction is necessary to produce the Cu_3Ti_3O phase at its interface with TiO. Thus, at the initial Cu_3Ti_3O/TiO interface,

$$\mathrm{Ti} + \frac{3}{2}\mathrm{Cu} + \frac{1}{2}\mathrm{TiO} \rightarrow \frac{1}{2}\mathrm{Cu_3Ti_3O} \qquad [4]$$

Note that Cu_3Ti_3O is produced from TiO, a product in Reaction [2], rather than from atomic oxygen that, by assumption, does not diffuse. This effectively couples Reactions [2] and [4], since TiO is both product and reactant. The summation of the reaction free energies for this reaction path is shown in Figure 14 and is again computed on a per mole Ti basis for each equation (Eqs. [2] and [4]). The details of this calculation are also shown in the Appendix.

Another consideration arises from the work of Kelkar and Carim,[9] which estimates the solubility of Al in Cu_3Ti_3O to be as high as 15 at. pct, along with the Al-profile measurements shown in Figure 7 which show a diffusion gradient. As a result, the Cu_3Ti_3O phase, at its interface with TiO, is likely to be nearly saturated in Al. Thus, in addition to Eq. [2], at the initial Cu_3Ti_3O/TiO interface,

$$\mathrm{Ti} + \mathrm{Cu} + \frac{1}{2}\mathrm{TiO} + \frac{1}{2}\mathrm{Al} \rightarrow \frac{1}{2}\mathrm{Cu_2AlTi_3O} \qquad [5]$$

and, within Cu_3Ti_3O,

$$\frac{1}{2}\mathrm{Cu_2AlTi_3O} + \frac{1}{2}\mathrm{Cu} \rightarrow \frac{1}{2}\mathrm{Cu_3Ti_3O} + \frac{1}{2}\mathrm{Al} \qquad [6]$$

This effectively couples these three reactions, since TiO and Cu_2AlTi_3O are both product and reactant phases. Defining the reaction free energy of Eq. [6] as ΔG_6, the free energy of reaction for Eqs. [2], [5], and [6] can be computed. Also, it can be shown that if the magnitude of ΔG_6 is negligible, then the sum of the reaction free energy for equations [2], [5], and [6] is identical to $\Delta G_{2\text{–}4}$. If Eq. [6] is viewed as a solution/dissolution reaction, it would follow that ΔG_6 is small enough to neglect within the context of this report. The magnitude of the reaction free energy for these alternate reaction paths differs markedly from that of Eqs. [2] and [3], which suggests that the product phases are not as stable as was once thought.

As the reaction layer grows in thickness, the Al produced in Reaction [2] diffuses through the TiO and Cu_2AlTi_3O phases. This reaction set is coupled through TiO and Cu_2AlTi_3O. Oxygen is provided to the Cu_3Ti_3O layer from TiO, which explains why the TiO layer is relatively thin; that is, it is consumed. Note also that, since it was assumed that oxygen does not diffuse, no growth can occur, by this mechanism, at the ABA/Cu_3Ti_3O interface. The question of oxygen diffusion remains an open one. Clever inert-marker experiments would be very helpful, in the future, to elucidate this mechanistic suggestion.

V. CONCLUSIONS

The work reported here has shown that a Ti-containing ABA reacts with and subsequently wets the basal plane of polished sapphire. A braze cycle that peaked at 1118 K for 360 seconds was shown to yield two oxides, TiO and Cu_3Ti_3O, that completely cover the sapphire surface. After cooling from the brazing cycle, a third oxide, Ti_2O, forms at isolated regions of the TiO interface with Cu_3Ti_3O. Heat treatment at 773 K causes further growth of this oxide, and it was suggested that Ti_2O grows as a result of the reaction between Ti and TiO. Since only minor volume changes result from this reaction, it was concluded that residual stress would not result in mechanical problems. Diffusion-like tails of Cu and Al were found in the Cu_3Ti_3O layer, but only local fluctuations of Ti were found. Coupled reactions were provided to suggest that growth of Cu_3Ti_3O occurs at its interface with TiO. Thermodynamic estimations suggest that the product phases are not as stable as the literature implies. The issue of the oxygen gradient in the reaction layer merits further study.

ACKNOWLEDGMENTS

We acknowledge the assistance of the following personnel at Sandia: W. Buttry, for Auger depth profile analysis; A. Kilgo, for metallographic sample preparation and analysis; and C. Walker, for furnace brazing of specimens. We also acknowledge the thorough review performed by P.T. Vianco of this laboratory. Sandia is a multiprogram laboratory operated by Sandia Corporation, a Lockheed Martin Company, for the United States Department of Energy's National Nuclear Security Administration under Contract No. DE-AC04-94Al85000.

APPENDIX

The work described in this article is part of a larger program of study to compare the effectiveness of the metals Ti, Zr, and Hf as braze alloy active constituents. Consequently, the stoichiometry in Eqs. [2] through [6] was written on a per mole Ti basis for comparison purposes. The reaction free energies for Eqs. [2] and [3] can be written as

$$\Delta G_2 = G_{\mathrm{TiO}} + \frac{2}{3}G_{\mathrm{Al}} - G_{\mathrm{Ti}} - \frac{1}{3}G_{\mathrm{Al_2O_3}} \qquad [A1]$$

and

$$\Delta G_3 = \frac{1}{3}G_{\mathrm{Cu_3Ti_3O}} - G_{\mathrm{Cu}} - G_{\mathrm{Ti}} - \frac{1}{6}G_{\mathrm{O_2}} \qquad [A2]$$

where G is the Gibbs free energy, listed in the work of Barin.[16] The only one not listed is $G_{Cu_3Ti_3O}$, which

is determined as follows. From the formation reaction described in Eq. [4], the unknown free energy can be written as

$$\frac{1}{3} G_{Cu_3Ti_3O} = \Delta G_4 + G_{Cu} + G_{Ti} + \frac{1}{6} G_{O_2} \qquad [A3]$$

where ΔG_4 is the reaction free energy of Cu_3Ti_3O and was estimated by Kelkar *et al.*[8] to be −170 kJ/mole of Ti. Substitution of Eq. [A3] into [A2] and summing Eqs. [A1] and [A2] yields

$$\Delta G_{2\text{-}3} = G_{TiO} + \frac{2}{3} G_{Al} - 170 - G_{Ti} - \frac{1}{3} G_{Al_2O_3}$$

and is plotted *vs* temperature in Figure 14. Using this same process for Eqs. [2] and [4] yields

$$\Delta G_{2\text{-}4} = \frac{1}{2} G_{TiO} - \frac{1}{2} G_{Ti} + \frac{2}{3} G_{Al} - \frac{1}{3} G_{Al_2O_3} + \frac{1}{4} G_{O_2} \frac{-3}{2}(170) \qquad [A4]$$

and this equation is also computed from the data of Barin[16] and plotted in Figure 14.

REFERENCE

1. P.T. Vianco, J.J. Stephens, P.F. Hlava, and C.A. Walker: *Welding J., Res. Suppl*. in press.
2. R.E. Loehman and A.P. Tomsia: *Acta Metall. Mater*., 1992, vol. 40, Suppl., pp. S75-S83.
3. J.H. Selverian, F.S. Ohuchi, and M.R. Notis: *Mater. Res. Soc. Symp*., 1990, vol. 167, pp. 335-40.
4. J.H. Selverian: Ph.D. Dissertation, Lehigh University, Bethlehem, PA, 1988.
5. S. Kang and J.H. Selverian: *J. Mater. Sci*., 1992, vol. 27, pp. 4536-44.
6. M.L. Santella, J.A. Horton, and J.J. Pak: *J. Am. Ceram. Soc*., 1990, vol. 73, pp. 1785-87.
7. A. Carim: *Scripta Metall. Mater*., 1991, vol. 25, pp. 51-54.
8. G.P. Kelkar, K.E. Spear, and A.H. Carim: *J. Mater. Res*., 1994, vol. 9 (9), pp. 2244-50.
9. G.P. Kelkar and A.H. Carim: *Mater. Lett.*, 1995, vol. 23, pp. 231-35.
10. H. Hao, Y. Wang, Z. Jin, and X. Wang: *J. Mater. Sci*., 1995, vol. 30, pp. 1233-39.
11. T. Ichimori, C. Iwamoto, and S. Tanaka: *Mater. Sci. Forum*, 1999, vol. 294 (6), pp. 337-40.
12. W.F. Chambers and J.H. Doyle: *SANDIA TASK8, version C: A Subroutined Electron Microprobe Automation System*, SAND90-1703, Sandia National Laboratories, Albuquerque, NM, 1990.
13. B.J. Lee and N. Saunders: *Z. Metallkd*., 1997, vol. 88, pp. 152-61.
14. *Binary Alloy Phase Diagrams*, T.B. Massalski, ed., ASM, Metals Park, OH, 1986.
15. P. Villers and L.D. Calvert: *Pearson's Handbook of Crystallographic Data for Intermetallic Phases*, 2nd ed., ASM INTERNATIONAL, Materials Park, OH, 1991, vol. 4.
16. I. Barin: *Thermodynamic Data of Pure Substances*, VCH Verlagsgesellschaft mbH, Weinheim, Federal Republic of Germany, 1989.